

antitumor immunity (8). Thus, linkage of tumor antigens with mDF2β enabled not only efficient APC targeting, but presumably also activated DC maturation in vivo. The importance of DC maturation in induction of adaptive immune responses has been recently suggested by a similar observation that linkage with agonistic DEC205-specific antigen facilitated efficient antigen uptake and processing by DCs, yet this construct induced tolerance unless DCs were first activated by CD40 engagement (19).

We report here that mDF2β, which has hitherto been considered a peptide with direct antimicrobial effects, modulates adaptive immune response not only by recruiting iDCs to the site of inflammation through chemokine receptor CCR6 (8, 9) but also by activating signaling for DC maturation through a microbial pattern recognition receptor, TLR-4. Our data suggest that mDF2β could be considered a so-called endogenous ligand of TLR-4 signaling as proposed, for example, for heat shock antigens Hsp60 and Hsp70 expressed during stress and/or necrosis (20, 21). Formally, the possibility remains that mDF2β may act as a potentiator of subthreshold amounts of LPS, tightly bound to it in a complex during defensin purification (14). The biological relevance of our finding remains to be elucidated. It is tempting to speculate that some β-defensins may function to counter suppressive microbial factors by generating more robust host inflammatory and T_H1 responses. Furthermore, we do not know yet whether mDF2β activates other subsets of immune cells, such as mature DCs, although our preliminary data suggest that it may activate the macrophage cell line RAW267 (14). Finally, the natural adjuvant property of mDF2β may also be utilized for the development of more effective vaccines and immunotherapeutics, for example, by targeting and/or recruiting iDCs in vivo, and at the same time, activating them to elicit potent T cell immunity (8, 10).

References and Notes

1. R. Medzhitov, C. Janeway Jr., *N. Engl. J. Med.* **343**, 338 (2000).
2. R. Medzhitov, C. A. Janeway Jr., *Curr. Opin. Immunol.* **9**, 4 (1997).
3. P. Matzinger, *Semin. Immunol.* **10**, 399 (1998).
4. S. D. Wright, R. A. Ramos, P. S. Tobias, R. J. Ulevitch, J. C. Mathison, *Science* **249**, 1431 (1990).
5. M. J. Sweet, D. A. Hume, *J. Leukoc. Biol.* **60**, 826 (1996).
6. Y. Tsutsumi-Ishii, I. Nagaoka, *J. Leukoc. Biol.* **71**, 154 (2002).
7. V. Toshchakov et al., *Nature Immunol.* **3**, 392 (2002).
8. A. Biragyn et al., *J. Immunol.* **167**, 6644 (2001).
9. D. Yang, et al., *Science* **286**, 525 (1999).
10. A. Biragyn et al., *Blood* **100**, 1153 (2002).
11. Materials and methods are available as supporting material on Science Online.
12. A. Biragyn et al., *Nature Biotechnol.* **17**, 253 (1999).
13. B. C. Schutte, P. B. McCray Jr., *Annu. Rev. Physiol.* **64**, 709 (2002).
14. A. Biragyn, unpublished data.
15. A. Wiese et al., *J. Membr. Biol.* **162**, 127 (1998).

16. B. W. Jarvis, H. Lichenstein, N. Qureshi, *Infect. Immun.* **65**, 3011 (1997).
17. C. J. da Silva, K. Soldau, U. Christen, P. S. Tobias, R. J. Ulevitch, *J. Biol. Chem.* **276**, 21129 (2001).
18. M. W. Hornef, T. Frisan, A. Vandewalle, S. Normark, A. Richter-Dahlfors, *J. Exp. Med.* **195**, 559 (2002).
19. D. Hawiger et al., *J. Exp. Med.* **194**, 769 (2001).
20. K. Ohashi, V. Burkart, S. Flohe, H. Kolb, *J. Immunol.* **164**, 558 (2000).
21. R. M. Vabulas et al., *J. Biol. Chem.* **277**, 15107 (2002).
22. We thank R. Gress (NCI/NIH), for critical discussion of the manuscript and helpful comments; N. Qureshi (Uni-

versity of Missouri) for the gift of RsDPLa; and B. Reis and C. Green (SAIC-Frederick) for proofreading. This publication has been funded in part with federal funds from the National Cancer Institute and National Institutes of Health, under contract No. NOL-CO-12400.

Supporting Online Material

www.sciencemag.org/cgi/content/full/298/5595/1025/DC1

Materials and Methods
Figs. S1 to S3

28 June 2002; accepted 30 August 2002

Cytoprotective Role of Ca²⁺-Activated K⁺ Channels in the Cardiac Inner Mitochondrial Membrane

Wenhong Xu,¹ Yongge Liu,² Sheng Wang,² Todd McDonald,³ Jennifer E. Van Eyk,³ Agnieszka Sidor,¹ Brian O'Rourke^{1*}

Ion channels on the mitochondrial inner membrane influence cell function in specific ways that can be detrimental or beneficial to cell survival. At least one type of potassium (K⁺) channel, the mitochondrial adenosine triphosphate-sensitive K⁺ channel (mitoK_{ATP}), is an important effector of protection against necrotic and apoptotic cell injury after ischemia. Here another channel with properties similar to the surface membrane calcium-activated K⁺ channel was found on the mitochondrial inner membrane (mitoK_{Ca}) of guinea pig ventricular cells. MitoK_{Ca} significantly contributed to mitochondrial K⁺ uptake of the myocyte, and an opener of mitoK_{Ca} protected hearts against infarction.

Sustained adenosine triphosphate (ATP) production by mitochondria requires maintenance of a large electrochemical gradient for protons across the mitochondrial inner membrane. This proton motive force is established by active proton pumping by the electron transport chain, producing both a pH gradient (ΔpH) and a mitochondrial transmembrane potential (ΔΨ_m). Because ΔΨ_m can be depolarized by energy-dissipating ion flux, the mitochondrial inner membrane was earlier assumed to have a low resting permeability to cations (1). However, it is well established that both divalent (2) and monovalent cation transport pathways (uniporters) are present on the inner membrane and that K⁺ conductance can be substantial in energized mitochondria (3, 4).

A growing body of evidence indicates that mitochondrial ATP-sensitive K⁺ channels (mitoK_{ATP}) are important determinants of resistance to ischemic damage (5, 6) and apoptosis (7) and may be clinically recruitable to prevent or mitigate cardiac or neuronal ischemic injury (8). To determine whether other

K⁺ channel subtypes are also present on the cardiac mitochondrial inner membrane, here we use direct single channel patch-clamp recordings of cardiac mitoplasts and mitochondrial K⁺ flux measurements to identify mitochondrial Ca²⁺-activated K⁺ channels (mitoK_{Ca}) as a component of the mitochondrial background K⁺ conductance, and we test whether mitoK_{Ca} confers protection against infarction in the intact heart.

Mitoplasts prepared from isolated cardiac myocytes were patch-clamped (9) to identify the major single channel conductances of the inner membrane. In K⁺ solutions (150 mM K⁺) containing 512 nM Ca²⁺, single channel currents with a full unitary conductance of 307 ± 4.6 pS (n = 4 of 17 single channel patches) were often observed, with openings frequently interrupted by transitions to sub-conductance states ranging from 24 to 161 pS (Fig. 1, A to C). When pipettes were back-filled with the K⁺ channel toxin charybdotoxin (ChTx; 200 nM) to permit slow diffusion of the toxin into the pipette tip, channel activity disappeared within 30 min, indicative of the probable presence of K_{Ca} channels (Fig. 1D). In some patches in 512 nM Ca²⁺, and particularly at higher bath Ca²⁺ concentrations, channel activity was too great to identify individual channel openings; in these cases, ensemble average patch currents were analyzed and shown to be reversibly increased by raising Ca²⁺ in the medium (Fig.

¹Institute of Molecular Cardiobiology, The Johns Hopkins University School of Medicine, Baltimore, MD 21205, USA. ²Maryland Research Laboratories, Otsuka Maryland Research Institute, Rockville, MD 20850, USA. ³Department of Physiology, Queen's University, Kingston, Ontario, K7L 3N6 Canada.

*To whom correspondence should be addressed. E-mail: bor@jhmi.edu.

1E). This activation by Ca^{2+} was eliminated when ChTx was present in the pipette (Fig. 1E). The ChTx-sensitive channels were unaffected by applying the $\text{mitoK}_{\text{ATP}}$ inhibitor 5-hydroxydecanoate (500 μM), excluding a contribution from $\text{mitoK}_{\text{ATP}}$, which was not expected to be activated under the experimental conditions (Fig. 1D).

To determine whether the K_{Ca} activity observed in single-channel recordings contributed significantly to the total K^+ influx of intact mitochondria, we performed K^+ concentration ($[\text{K}^+]$) jump experiments in isolated cardiac myocytes loaded with the K^+ -selective fluorescent indicator PBF1 (9), with the loading protocol optimized to achieve preferential labeling of the mitochondrial matrix (Fig. 2A). Although K_{Ca} channels are not believed to be present on the surface membranes of ventricular myocytes, we took the further precaution of permeabilizing the surface membrane with saponin to eliminate potential complications associated with K^+ flux across the sarcolemma or signal contamination from cytosolic PBF1 during wide-field fluorescence imaging. Using a rapid switching device capable of changing solutions in <2 s (Fig. 2B), we increased bath $[\text{K}^+]$ from 0 to 5 mM, and we determined net K^+ flux into the matrix as the change in the fluorescence excitation ratio of PBF1 (340/380

nm). The response to K^+ was reversible and reproducible (Fig. 2C) and was accelerated, as expected, by the K^+ ionophore valinomycin (3). In paired experiments, 100 nM ChTx slowed the time constant of mitochondrial K^+ uptake by 8- to 10-fold (Fig. 2, D and E). The rate of K^+ influx was also inhibited by the K^+ channel blockers Ba^{2+} and quinine (Fig. 2E), known inhibitors of surface membrane K_{Ca} channels (10, 11) that also block K^+ influx into isolated mitochondria (12, 13).

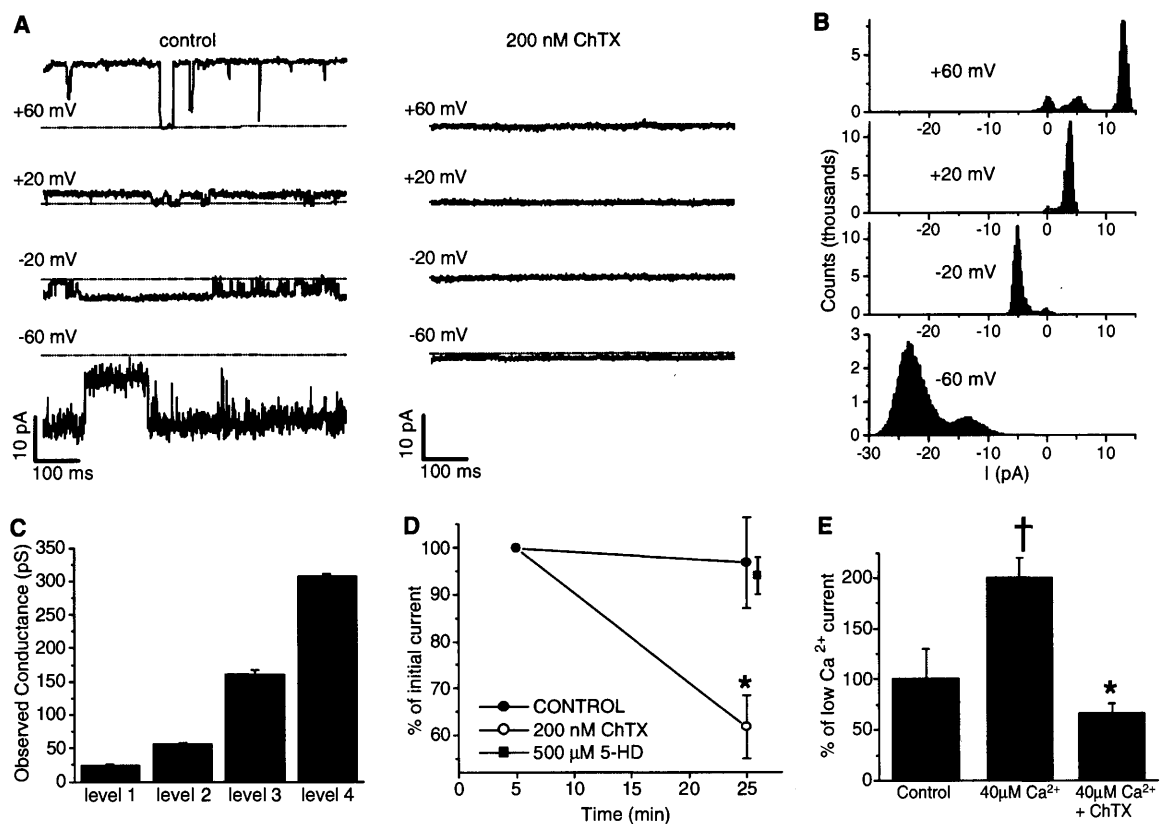
As ChTx has been shown to block several K_{Ca} subtypes and may also inhibit voltage-gated K^+ channels of the $\text{Kv}1.3$ type, we also tested the efficacy of iberiotoxin, which is selective for large conductance K_{Ca} channels of the BK subtype (14). Similar to ChTx, iberiotoxin (100 nM), slowed the time constant of K^+ influx by about 146%, indicating a contribution from large conductance K_{Ca} channels (Fig. 2E). We further confirmed the involvement of the large conductance K_{Ca} channel by using the K_{Ca} opener NS-1619. This compound opens the BK $_{\text{Ca}}$ subtype of surface membrane K_{Ca} without affecting small- or intermediate-conductance K_{Ca} family members (15). Mitochondrial K^+ uptake was accelerated about twofold by NS-1619 (Fig. 2F).

To determine whether K_{Ca} channel proteins were present in mitochondrial mem-

branes, we performed immunoblot analysis on mitochondria from isolated myocytes (9). Immunostaining of intact myocyte proteins with an antibody against the surface membrane BK_{Ca} channel showed at least two major bands of about 55 and 220 kD (Fig. 3A). In contrast, a single protein band of about 55 kD, similar to the predicted size of the α subunit of K_{Ca} , was evident for an equal amount of mitochondrial protein.

We used a highly purified liver mitochondrial inner membrane preparation to more rigorously confirm the mitochondrial localization of the BK_{Ca} immunoreactive protein. On a one-dimensional gel, BK_{Ca} antibody staining showed a prominent band at about 80 kD and two fainter bands in the 50- to 75-kD range (Fig. 3C) displaceable by control antigen (Fig. 3B). Further separation of the mitochondrial proteins by two-dimensional polyacrylamide gel electrophoresis (PAGE) (pH 3 to 10; 10% SDS) revealed a plethora of mitochondrial inner membrane proteins by silver staining (Fig. 3D). In the range of pH 5 to 7.5, 40 to 85 kD, the most prominent spot was the mitochondrial ATP synthase β chain (~ 56 kD), which we used as a landmark for the subsequent immunoblot analysis (Fig. 3D). The antibody to BK_{Ca} specifically labeled a protein spot of ~ 80 kD that was clearly separated from the ATP synthase by virtue

Fig. 1. ChTx-sensitive channels in cardiac mitoplasts. (A) Single channel recording of a 300-pS channel within minutes of making the gigaohm seal (control) and 30 min later (200 nM ChTx) after toxin diffusion into the tip. (B) Amplitude histograms of the full and subconductance openings for the patch shown in (A). (C) Mean conductance levels for 17 single channel patches. Transitions between levels were commonly observed within the same recordings. (D) Inhibition of mitoplast ensemble average currents (at -60 mV) by ChTx. Paired currents were normalized to initial levels recorded within the first 5 min of the experiment. Currents were reported without correction for leak current across the seal, thus underestimating the fraction of total current attributable to ChTx-sensitive channels. Filled square denotes currents 20 to 30 min after the addition of 5-hydroxydecanoate (5-HD; normalized to pre-5HD control). (E) Effect of increasing bath free $[\text{Ca}^{2+}]$ from 512 nM to 40 μM for patches with or without 200 nM ChTx. Paired t test: * $P < 0.05$, † $P < 0.01$, versus control.



REPORTS

of its charge differential in the isoelectric focusing dimension (pH 5 to 7.5 gradient).

The opening of the mitoK_{ATP} channel plays an important role in protecting hearts against ischemic damage; therefore, we reasoned that activating K_{Ca} channels might similarly protect hearts against infarction. We subjected perfused hearts to global ischemia and reperfusion after pretreatment with NS-1619 in the presence or absence of the K_{Ca} antagonist paxilline (9, 15). Left ventricular

developed pressure (LVP) and heart rate were unchanged during the 5- to 10-min exposure to the K_{Ca} channel compounds (Table 1). As expected from the cross-reactivity of the K_{Ca} opener with the vascular surface membrane isoform of the channel, NS-1619 initially increased coronary flow by 24% at 10 μM and 66% at 30 μM during exposure. This increase in flow was blocked by coapplication with paxilline, which had no effect on flow in the absence of the opener. We applied global

ischemia to eliminate coronary flow as a factor during the ischemic phase [see comments on selectivity in (9)]. No significant difference between groups in heart rate or flow was evident after reperfusion (Table 1). LVP was better preserved in the NS-1619-treated groups; however, this difference did not reach statistical significance. A 5-min preischemic exposure to 30 μM NS-1619 approximately halved the extent of myocardial infarction, a level of protection similar to that reported for the mitoK_{ATP} channel opener diazoxide in the same infarction model (16) (Fig. 4). For 10 μM NS-1619, no protection was observed for a 5-min pretreatment, but extending the exposure time to 10 min resulted in protection in four of six hearts (Fig. 4). Paxilline alone had no effect on infarct size, but it completely blocked the protection afforded by 30 μM NS-1619.

The results indicate that an isoform of the large conductance K_{Ca} exists on the mitochondrial inner membrane and constitutes a large fraction of K⁺ uniport activity. MitoK_{Ca}-mediated current was detectable at cytosolic Ca²⁺ concentrations in the range of resting Ca²⁺ in the myocyte (~200 nM; see Fig. 2) and enhanced at high cytosolic Ca²⁺ concentrations (Fig. 1E). Because the ChTx-sensitive current in mitoplast-attached patches increased when Ca²⁺ outside the pipette was raised, the relevant regulatory site for Ca²⁺ on the channel is likely to face the mitochondrial matrix. MitoK_{Ca} would then be activated as matrix Ca²⁺ rises in response to an increase in the average cytosolic Ca²⁺ load, such as occurs during an increase in cardiac work or ischemia. Thus, mitoK_{Ca} may play an important role both in modulating bioenergetics under physiological conditions and during conditions of Ca²⁺ overload.

The function of mitoK_{Ca} may be to improve the efficiency of mitochondrial energy production. K⁺ is required for optimal functioning of oxidative phosphorylation (17) and may also modulate other mitochondrial functions, such as reactive oxygen species production. The mitochondrial K⁺ cycle, involving electrophoretic K⁺ uptake and electroneutral K⁺/H⁺ exchange, is important for mitochondrial volume regulation (4); this too can influence substrate oxidation (18). Analogously, the activation of mitoK_{ATP} improves ATP production (19), dampens mitochondrial Ca²⁺ accumulation during ischemia (20, 21), and alters the rate of mitochondrial reactive oxygen species production (22, 23), the latter leading to the activation of intracellular signaling pathways (24). The present finding, that activating a completely different class of mitochondrial K⁺ channel confers a similar degree of protection, independently confirms that mitochondrial K⁺ influx is an important factor in mitigating injury, a

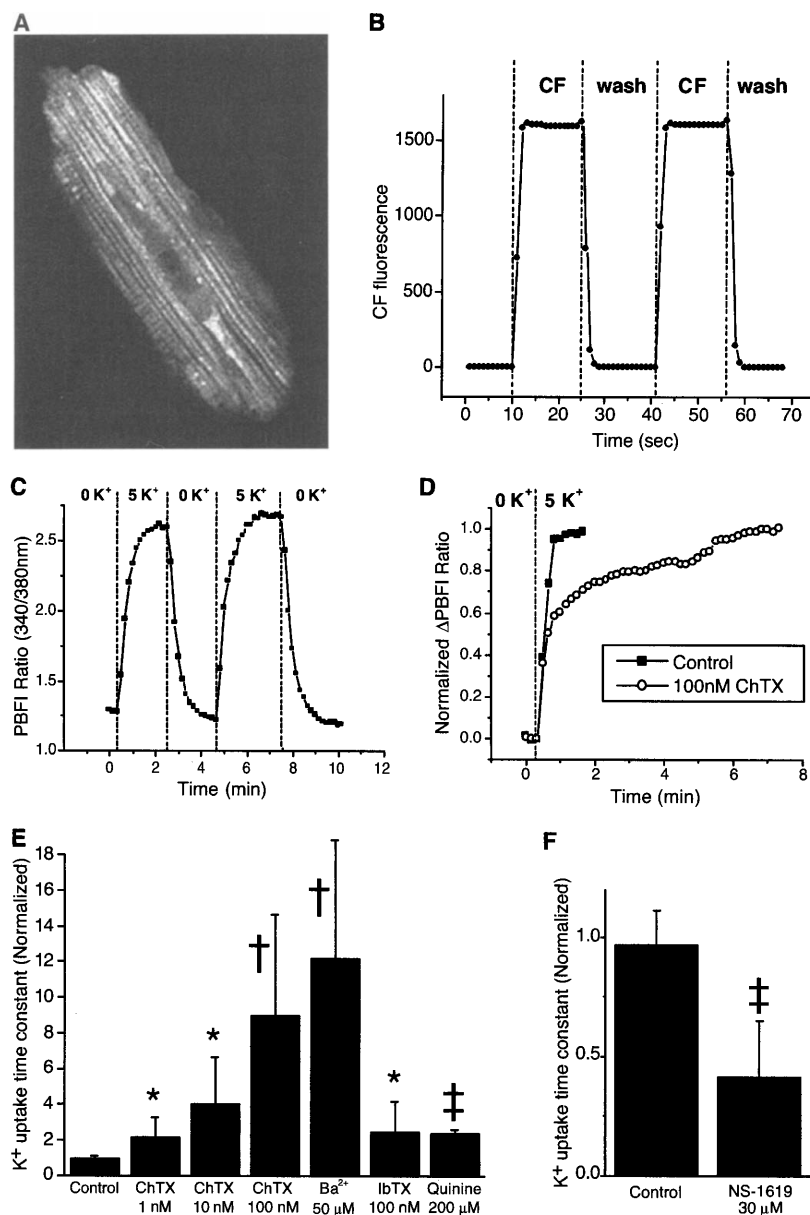


Fig. 2. Effects of K_{Ca} inhibition on mitochondrial K⁺ uptake. (A) Pattern of PBFI fluorescence indicated preferential mitochondrial loading of the dye, which was retained upon saponin permeabilization. (B) Rapid exchange of the bathing medium confirmed by superfusion and washout of 100 μM carboxyfluorescein (CF). (C) Concentration jumps from 0 to 5 mM K⁺ accompanied by a reproducible increase in mitochondrial matrix PBFI excitation ratio (F₃₄₀/F₃₈₀ nm), permitting paired experiments within a field containing five to eight myocytes. (D) Inhibition of K⁺ uptake in the presence of 100 nM ChTx. ChTx slowed K⁺ uptake by ~20-fold in the experiment shown. (E) Summary of the effects of K_{Ca} channel inhibitors on the time constant of mitochondrial K⁺ uptake. Inhibition of K⁺ uptake depended on ChTx concentration and was also affected by Ba²⁺, Iberitoxin, and quinine. (F) The BK_{Ca} channel opener NS-1619 accelerated the rate of K⁺ uptake by more than twofold. Paired *t* test: **P* < 0.05, †*P* < 0.01, ‡*P* < 0.001 versus control.

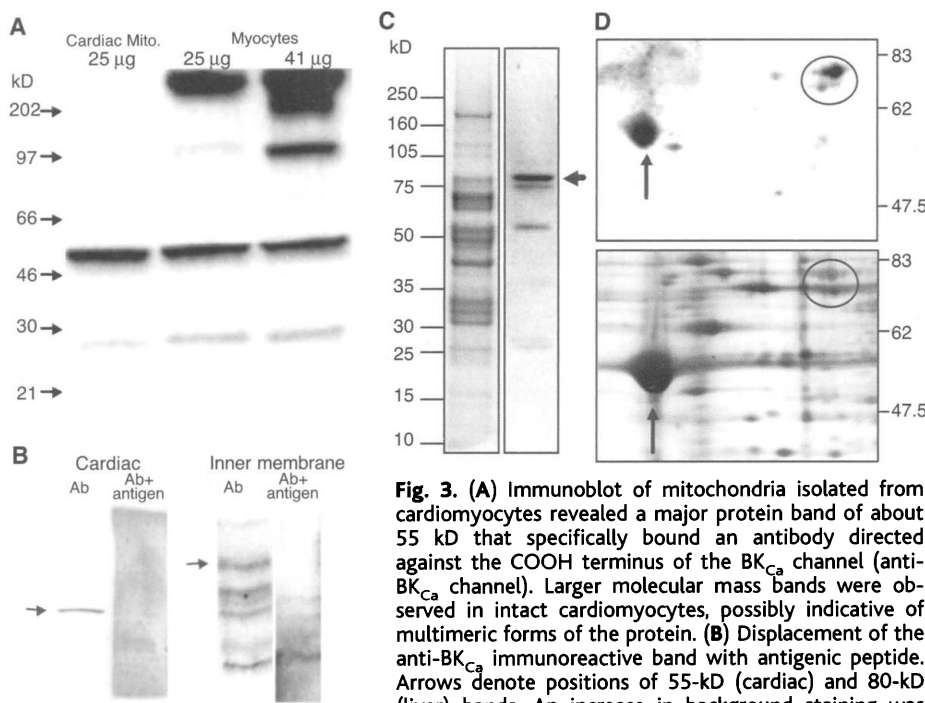


Fig. 3. (A) Immunoblot of mitochondria isolated from cardiomyocytes revealed a major protein band of about 55 kD that specifically bound an antibody directed against the COOH terminus of the BK_{Ca} channel (anti-BK_{Ca} channel). Larger molecular mass bands were observed in intact cardiomyocytes, possibly indicative of multimeric forms of the protein. (B) Displacement of the anti-BK_{Ca} immunoreactive band with antigenic peptide. Arrows denote positions of 55-kD (cardiac) and 80-kD (liver) bands. An increase in background staining was evident when antigen was present. (C) One-dimensional PAGE of liver mitochondrial inner membrane (10 µg) stained with Gel Code blue (left) or antibody to BK_{Ca} (right). (D) Enlarged region (pH 5 to 7.5 zone) of a two-dimensional polyacrylamide (pH 3 to 10; 10% SDS-PAGE) silver-stained gel (lower) and its corresponding immunoblot (upper), performed sequentially, first with the antibody to BK_{Ca} and then with antibody to ATP synthase β chain. Spots identified as BK_{Ca} are circled and the ATP synthase β chain is indicated by arrows.

Cardiac hemodynamics and coronary flow during control perfusion, NS-1619 application, and post-reperfusion. Details are as described in (9). Values listed under drug and reperfusion were obtained at the end of drug perfusion and at the end of the 2-hour reperfusion, respectively.

	Baseline	Drug	Reperfusion
<i>LVP (mmHg)</i>			
Control	104 ± 9		34 ± 6
NS-1619 (10 µM)	110 ± 5	104 ± 5	41 ± 6
NS-1619 (30 µM)	108 ± 3	93 ± 1	56 ± 5
NS + paxilline	103 ± 14	88 ± 9	33 ± 10
Paxilline	113 ± 4	111 ± 3	33 ± 5
<i>Heart rate (beats/min)</i>			
Control	180 ± 8		157 ± 7
NS-1619 (10 µM)	186 ± 12	189 ± 21	157 ± 12
NS-1619 (30 µM)	183 ± 9	183 ± 12	133 ± 9
NS + paxilline	180 ± 7	168 ± 9	148 ± 9
Paxilline	167 ± 5	160 ± 7	147 ± 5
<i>Coronary flow (ml/min)</i>			
Control	43 ± 6		18 ± 2
NS-1619 (10 µM)	42 ± 5	52 ± 6*	21 ± 3
NS-1619 (30 µM)	35 ± 5	58 ± 6*	19 ± 2
NS + paxilline	48 ± 3	54 ± 3	21 ± 5
Paxilline	51 ± 4	51 ± 3	16 ± 1

*P < 0.05 versus baseline value.

conclusion that has been difficult to prove unequivocally for mitoK_{ATP} with diazoxide because of the potentially confounding nonspecific effects of the drug at high concentrations (25).

Mitochondrial K⁺ uptake is increased by energization (3, 26) and Ca²⁺ (13) in isolated

mitochondria, but the molecular identity of the uniporter is unknown. Interestingly, the size of the mitoK_{Ca} channel monomer is similar to other putative mitochondrial K⁺ channels. Several proteins in the same molecular size range (50 to 60 kD) were purified from mitochondria with a quinine affinity column

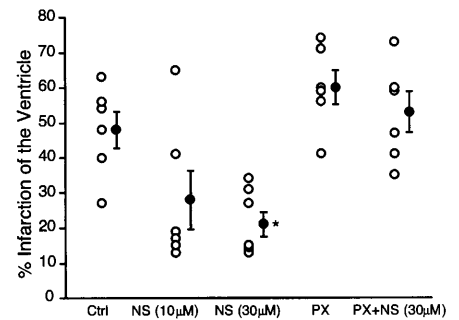


Fig. 4. Effect on myocardial infarct size. Open circles, infarct size of individual hearts; filled circles, mean and standard errors of the group. Ctrl, untreated controls with 30-min global ischemia and 2-hour reperfusion; NS (10 µM), hearts treated with 10 µM NS-1619 for 10 min before ischemia; NS (30 µM), hearts treated with 30 µM NS-1619 for 5 min before ischemia; PX, hearts treated for 5 min with 1 µM paxilline before ischemia; PX+NS (30 µM), hearts treated with a combination of 1 µM paxilline and 30 µM NS-1619 for 5 min before ischemia. *P < 0.05.

and confer K⁺ channel activity upon reconstitution (27, 28); similarly, a 54-kD protein was tentatively identified as a component of mitoK_{ATP} (29). The sensitivity of such reconstituted channels to K⁺ channel toxins and their potential immunoreactivity with antibodies to BK_{Ca} remain to be investigated. Excluding mitoK_{ATP}, which would not be active under energized conditions, the present findings are the only ones known to link mitochondrial K⁺ flux to a specific mitochondrial K⁺ channel. K_{Ca} channels have been reported in glioma cell mitoplasts (30), but their contribution to K⁺ flux and their physiological role were not explored.

In summary, the present findings identify mitoK_{Ca} in cardiac mitochondria, demonstrate that it contributes to mitochondrial K⁺ uniporter conductance, and assign a role for mitoK_{Ca} in protection against ischemic injury.

References and Notes

1. P. Mitchell, *Nature* **191**, 144 (1961).
2. M. J. Selwyn, A. P. Dawson, S. J. Dunnett, *FEBS Lett.* **10**, 1 (1970).
3. D. W. Jung, E. Chavez, G. P. Brierley, *Arch. Biochem. Biophys.* **183**, 452 (1977).
4. K. D. Garlid, *Biochim. Biophys. Acta* **1275**, 123 (1996).
5. Y. Liu, T. Sato, B. O'Rourke, E. Marban, *Circulation* **97**, 2413 (1998).
6. K. D. Garlid et al., *Circ. Res.* **81**, 1072 (1997).
7. M. Akao, A. Ohler, B. O'Rourke, E. Marban, *Circ. Res.* **88**, 1267 (2001).
8. J. G. Shake et al., *Ann. Thorac. Surg.* **72**, 1849 (2001).
9. Materials and methods are available as supporting material on Science Online.
10. G. Perez, A. Lagrutta, J. P. Adelman, L. Toro, *Biophys. J.* **66**, 1022 (1994).
11. C. B. Ransom, H. Sontheimer, *J. Neurophysiol.* **85**, 790 (2001).
12. J. J. Diwan, *J. Membr. Biol.* **84**, 165 (1985).
13. A. P. Halestrap, P. T. Quinlan, D. E. Whipps, A. E. Armston, *Biochem. J.* **236**, 779 (1986).
14. K. M. Giangiaccomo et al., *Biochemistry* **32**, 2363 (1993).

15. V. K. Gribkoff *et al.*, *Mol. Pharmacol.* **50**, 206 (1996).
 16. T. Miura, Y. Liu, H. Kita, T. Ogawa, K. Shimamoto, *J. Am. Coll. Cardiol.* **35**, 238 (2000).
 17. G. A. Kimmich, H. Rasmussen, *Biochim. Biophys. Acta* **131**, 413 (1967).
 18. A. P. Halestrap, *Biochim. Biophys. Acta* **973**, 355 (1989).
 19. A. J. Kowaltowski, S. Seetharaman, P. Paucek, K. D. Garlid, *Am. J. Physiol. Heart Circ. Physiol.* **280**, H649 (2001).
 20. M. Murata, M. Akao, B. O'Rourke, E. Marban, *Circ. Res.* **89**, 891 (2001).
 21. L. Wang *et al.*, *Am. J. Physiol. Heart Circ. Physiol.* **280**, H2321 (2001).
 22. Z. Yao *et al.*, *Am. J. Physiol. Heart Circ. Physiol.* **277**, H2504 (1999).
 23. R. A. Forbes, C. Steenberg, E. Murphy, *Circ. Res.* **88**, 802 (2001).
 24. T. Pain *et al.*, *Circ. Res.* **87**, 460 (2000).
 25. T. Grimmsmann, I. Rustenbeck, *Br. J. Pharmacol.* **123**, 781 (1998).
 26. R. G. Hansford, A. L. Lehninger, *Biochem. J.* **126**, 689 (1972).
 27. R. Paliwal, G. Costa, J. J. Diwan, *Biochemistry* **31**, 2223 (1992).
 28. J. J. Diwan, T. Haley, D. R. Sanadi, *Biochem. Biophys. Res. Commun.* **153**, 224 (1988).
 29. P. Paucek *et al.*, *J. Biol. Chem.* **267**, 26062 (1992).
 30. D. Siemen, C. Loupatatzis, J. Borecky, E. Gulbins, F. Lang, *Biochem. Biophys. Res. Commun.* **257**, 549 (1999).
 31. Supported by NIH R01HL54598 (B.O.R.) and CIHR 49843 (J.V.E.). We thank P. L. Pedersen and Y. H. Ko for the liver submitochondrial particles and M. Aon and E. Marbán for helpful comments.

Supporting Online Material

www.sciencemag.org/cgi/content/full/298/5595/1029/DC1.

Materials and Methods

24 May 2002; accepted 12 September 2002

Hijacking of Host Cell IKK Signalosomes by the Transforming Parasite *Theileria*

Volker T. Heussler,^{1*}† Sven Rottenberg,^{1*} Rebekka Schwab,¹ Peter Küenzi,¹ Paula C. Fernandez,¹ Susan McKellar,² Brian Shiels,² Zhijian J. Chen,³ Kim Orth,³ David Wallach,⁴ Dirk A. E. Dobbelaere^{1,‡}

Parasites have evolved a plethora of mechanisms to ensure their propagation and evade antagonistic host responses. The intracellular protozoan parasite *Theileria* is the only eukaryote known to induce uncontrolled host cell proliferation. Survival of *Theileria*-transformed leukocytes depends strictly on constitutive nuclear factor kappa B (NF-κB) activity. We found that this was mediated by recruitment of the multisubunit IκB kinase (IKK) into large, activated foci on the parasite surface. IKK signalosome assembly was specific for the transforming schizont stage of the parasite and was down-regulated upon differentiation into the nontransforming merozoite stage. Our findings provide insights into IKK activation and how pathogens subvert host-cell signaling pathways.

the NF-κB pathway in *Theileria*-transformed cells results in rapid apoptosis (7). Although the biological relevance of constitutive NF-κB activity in the survival of *Theileria*-transformed leukocytes is obvious, the way in which the parasite induces NF-κB activation is still unknown.

In contrast to most other apicomplexan parasites, which are enclosed in parasitophorous vacuoles, *Theileria* schizonts inhabit the host cell cytoplasm (8), where they are exposed to the cytosol and cytoskeleton of the infected cell. Several drugs, described in other systems to interfere with upstream components of the NF-κB activation cascade, fail to block *Theileria*-induced NF-κB activity (9), suggesting that the parasite might short-circuit the NF-κB activation pathway. We performed dual-staining confocal immunofluorescence microscopy using antibodies directed against a parasite surface protein, PIM, in combination with antibodies directed against subunits of the IKK complex (Fig. 1). Surprisingly, we found the *T. parva* schizont to be decorated with macromolecular foci detected by antibodies to IKK1 (Fig. 1A), IKK2, and NEMO (fig. S1). The number of IKK foci clustered at the parasite surface correlated with the size of the schizont, which can differ considerably from cell to cell. In addition, the size of the foci varied from structures that were barely detectable by light microscopy to particles with an apparent diameter of several hundred nanometers. V5-epitope-tagged forms of bovine IKK1, IKK2, or NEMO expressed in *T. parva*-transformed T cells became incorporated into the parasite-associated foci (shown for IKK2 in Fig. 1B), demonstrating that the foci can accommodate the different bovine IKK components. IKK foci could also be detected in *T. parva*-transformed B cells, as well as in monocyte/macrophage-derived cell lines and B cell lines transformed by *T. annulata* (Fig. 2).

The IKK complex is often referred to as the "IKK signalosome" because of its size (10), but activated signalosomes have not been visualized so far. Using in vitro kinase assays, we detected robust IKK activity in *T. parva*-transformed T cells (11). More importantly, phospho-specific antibodies readily detected phosphorylated forms of IKK (P-

Theileria parva and *Theileria annulata* are tick-transmitted protozoan parasites of cattle that cause severe lymphoproliferative diseases in large areas of Africa and Asia. Unprotected animals that become infected almost invariably succumb to theileriosis. *Theileria* spp. are closely related to other apicomplexan parasites, such as *Plasmodium*, *Toxoplasma*, and *Babesia* spp. The intracellular schizont stages of *T. parva* and *T. annulata* possess the capacity to transform the target host cells they infect. *T. parva* transforms T cells or B cells, whereas *T. annulata* induces uncontrolled proliferation of cells of monocyte/

macrophage lineage and B cells. The pronounced pathology and mortality caused by *Theileria* infections is tightly associated with the parasite's transforming capacity. *Theileria*-transformed cells acquire a metastatic phenotype, allowing them to proliferate in nonlymphoid as well as lymphoid host tissues, and also to form tumors when injected into immunocompromised mice (1).

Among its many functions, the transcription factor NF-κB also contributes to the regulation of genes that prevent apoptosis (2). Stimuli that trigger NF-κB activation all converge onto a multisubunit kinase complex called IKK (IκB kinase) that consists of two catalytic subunits, IKK1 (IKKα) and IKK2 (IKKβ), and a modulating subunit NEMO (IKKγ). IKK phosphorylates IκBs, the cytoplasmic inhibitors of NF-κB, tagging them for proteasomal degradation, thus allowing NF-κB to translocate to the nucleus (3). In *Theileria*-transformed cells, NF-κB is constitutively activated in a parasite-dependent manner (4, 5). This results in the expression of a number of κB-dependent genes, including several anti-apoptotic genes such as c-FLIP, c-iap, and xiap (6). Interference with

¹Division of Molecular Pathology, Institute of Animal Pathology, University of Bern, CH-3012 Bern, Switzerland. ²Department of Veterinary Parasitology, University of Glasgow, Glasgow G61-1QH Scotland. ³Department of Molecular Biology, University of Texas Southwestern Medical Center, Dallas, TX 75390-9148, USA. ⁴Department of Biological Chemistry, Weizmann Institute of Science, Rehovot, 76100, Israel.

*These authors contributed equally to this work.
 †Present address: Berhard-Nocht-Institute for Tropical Medicine, D-20359 Hamburg, Germany.
 ‡To whom correspondence should be addressed: E-mail: dirk.dobbelaere@itpa.unibe.ch